Simulation of antireflective subwavelength grating structures for optical device applications

Y. M. Song and Y. T. Lee

[1] Department of Information and Communications, Gwangju Insititute of Science and Technology, 1 Oryong-dong, Buk-gu, Gwangju 500-712, Republic of Korea

***Abstract*- Diffraction efficiencies of three different types of subwavelength grating (SWG) structures were simulated for optoelectronic device applications using rigorous coupled wave analysis method. The effect of height and period of SWG structures on the reflectance were investigated. Also, the internal and external reflection from the SWG structures were simulated and analyzed.**

I. INTRODUCTION

The phenomenon of antireflection is widely used to reduce optical losses at the interface between different optical media. Multi-layer coatings are commonly used on various optical devices, such as solar cells, photodetectors, displays and viewing glasses, to suppress undesired reflections. However, thin film technology has inherent problems such as adhesion, thermal mismatch, and the stability of the thin film stack [1]. Recently, subwavelength grating (SWG) structures have been considered as a promising candidate for high-efficiency optical devices due to their antireflection properties [2-4]. The grating structures, which has a shorter period than the wavelength of incident light, act as a homogeneous medium with an effective refractive index determined by the fill factor. Therefore, Fresnel reflection can be reduced significantly by SWG structures with a continuous effective index profiles. To obtain broadband antireflection property, SWG patterns should have tapered profile, such as pyramidal and conical shape, with taller height. However, it is clear that perfect cone or pyramid with very tall features would be costly in most of optical devices. In this study, we have simulated the diffraction efficiency of the three kinds of SWG structures, i.e., nanorod, truncated cone and perfect cone. Optimum structures are discussed in terms of reflectance and grating structures, such as height and period.

II. SIMULATION RESULTS AND DISCUSSION

Fig. 1 show schematic illustrations of SWG structures on GaAs in a shape of (a) nanorod, (b) truncated cone and (c) perfect cone. In a simulation, the period is 300 nm and the height varies from 0 to 800 nm. To enlarge the packing density, 6-fold hexagonal symmetry was used, and the distance between each pillars were fixed to 10% of the period. The apex diameter is 50% of the base diameter in the truncated cone. The theoretical calculations of reflectance were done by using the rigorous coupled-wave analysis (RCWA) method proposed by Moharam [5].

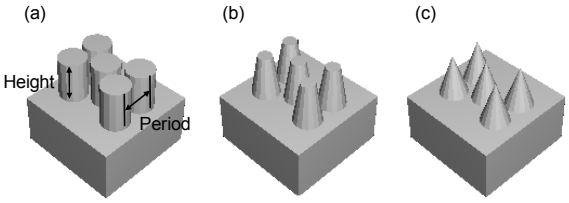

Fig. 1. Schematic illustrations of SWG structures on GaAs in a shape of (a) nanorod, (b) truncated cone, and (c) perfect cone used in simulation.

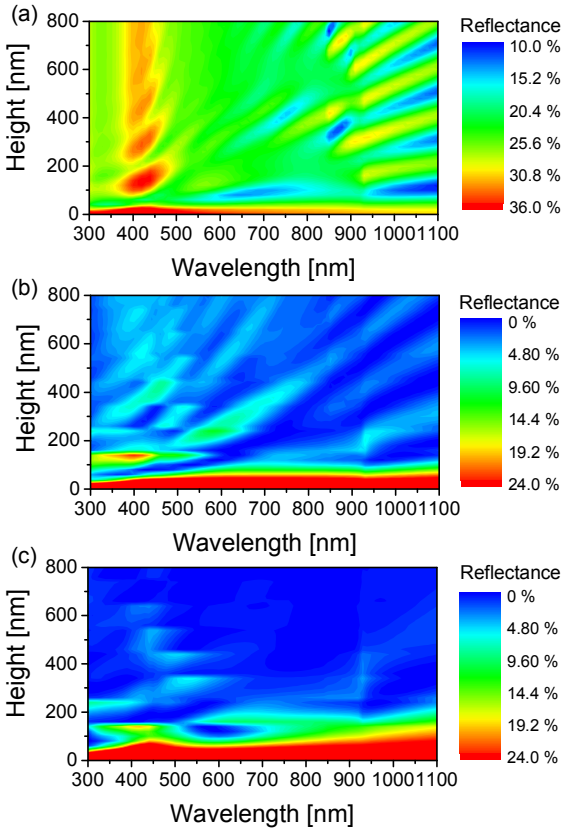

Fig. 2. Contour plot of the variation of reflectance of (a) nanorod, (b) truncated cone and (c) perfect cone as a function of cone height and wavelength for a 300 nm period of the array.

Figure 2 shows the contour plot of the variation of reflectance of (a) nanorod, (b) truncated cone and (c) perfect cone as a function of cone height and wavelength for a 300

nm period of the array. In case of nanorod structure, because the nanorod acts as an effective medium that approximates a single layer thin film, interference of reflections from the top and bottom of the layers causes the maxima and minima seen as pillar height is increased. This design is far from ideal for broadband applications due to higher reflection than that of conical shape. As shown in Fig. 2 (b) and (c), the conical shape has lower reflectance than the case of plat surface or nanorod case. Moreover, the perfect cone provides very low reflectance over a wide spectral range at cone heights above 500 nm. Even though the truncated cone has higher reflectance than the perfect cone, it has some specific region, which has very low reflectance, at cone heights below ~ 250 nm. This means that, for a specific application there are no need the perfect cone, which cause complex process steps. The cone height and shape can be chosen according to this plot.

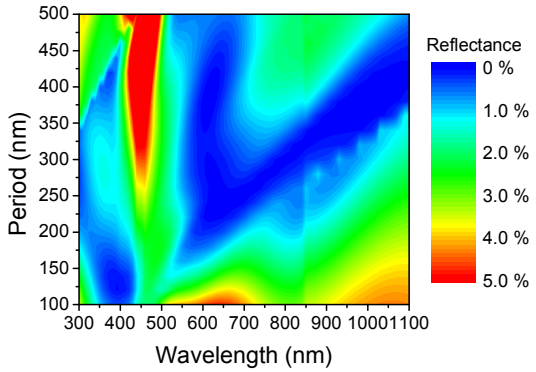

Fig. 3. Contour plot of the influence of period of the cone array on the reflectance as a function of wavelength for height of 450 nm.

Figure 3 shows the influence of the period of the array on the reflectance as a function of the wavelength for height of 450 nm. As expected, the low reflectance band broadens and shifts towards a higher wavelength region as the period of the array is increased. For periods above 300 nm, the band splits into two bands with reflectance of < 0.5%, including a band which is independent of the period of 200-450 nm at wavelength around 610 nm. This implies that low reflectance in a specific wavelength range can be obtained by adjusting the cone height without changing its period.

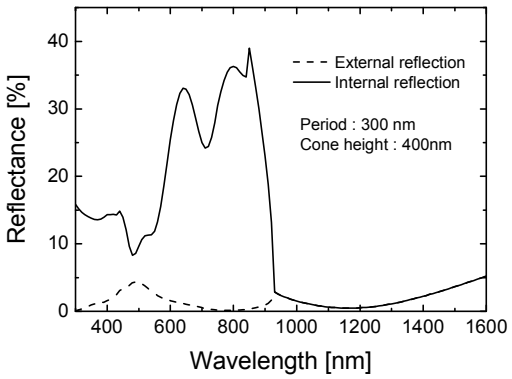

Fig. 4. Reflectance for both external (dash line) and internal reflection (solid line) as a function of wavelength for the period of 300 nm and height of 400nm.

Some optical devices such as light-emitting diodes and display panels emit light from inside to outside. In that case, the internal reflection, which means the refractive index of the incident medium is higher than that of transmitting medium, should be considered. When light is incident on SWG structures with period Λ, the angles of the transmitted diffraction waves $\theta_{t,m}$ in the m-th diffraction order are given by the grating equation,

$$\sin\theta_{t,m} = \frac{m\lambda}{\Lambda n_2} + \frac{n_1}{n_2}\sin\theta_i \qquad (1)$$

where n_1 and n_2 are the refractive indices of the incident and the transmitting medium, respectively, θ_i is the incidence angle, and λ is the incident wavelength. In external reflection, if the period of the diffraction grating becomes much smaller than the optical wavelength, only zeroth order is allowed to propagate. Unlike the external reflection, it is difficult to satisfy the zeroth order condition in the internal reflection due to higher refractive index of incident medium. Figure 4 shows the reflectance in case of internal and external reflection versus wavelength. As shown in Fig. 4, antireflection properties of < 5% were obtained at wavelength above ~900 nm. Higher order diffractions, however, occur at wavelength below ~900 nm in the internal reflection, which significantly increase the total reflectance. Hence, to obtain low reflectance in light emitting devices the period of the diffraction grating should be much shorter than the case of external reflection.

III. CONCLUSION

Three kinds of subwavelength grating structures on GaAs used to simulate the diffraction efficiency and the structural optimization were discussed for optical device applications. From the contour plots, the effects of the pillar heights and periods on the reflectance were also analyzed. The comparison between internal and external reflection was conducted to find out the optimum in light emitting devices.

ACKNOWLEDGMENT

This research was supported by the IT R&D program of MKE/IITA [2007-F-045-03].

REFERENCES

[1] P. Lalanne, and G. M. Morris, “Design, fabrication and characterization of subwavelength periodic structures for semiconductor anti-reflection coating in the visible domain,” *Proc. SPIE*, vol. 2776, pp. 300-309, 1996.

[2] Y. Kanamori, M. Sasaki, and K. Hane, “Broadband antireflection gratings fabricated upon silicon substrate,” *Opt. Lett.*, vol. 24, pp. 1422-1424, 1999.

[3] Z. Yu, H. Gao, W. Wu, H. Ge, and S. T. Chou, “Fabrication of large area subwavelength antireflection structures on Si using trilayer resist nanoimprint lithography and liftoff,” *J. Vac. Sci. Technol. B*, vol. 21, pp. 2874-2877, 2003.

[4] C. C. Striemer and P. M. Fauchet, “Dynamic etching of silicon for broadband antireflection applications,” *Appl. Phys. Lett.*, vol. 81, pp. 2980-2982, 2002.

[5] M. G. Moharam, “Coupled-wave analysis of two-dimensional dielectric gratings,” *Proc. SPIE*, vol 883, pp. 8-11, 1988.